

Soft-x-ray absorption spectroscopy of heterostructured high- T_c superconducting nanohybrids: $X\text{-Bi}_2\text{Sr}_2\text{CaCu}_2\text{O}_8$ [$X=\text{I}$, HgI_2 , and $(\text{Py-CH}_3)_2\text{HgI}_4$]

J. M. Chen,^{1,*} S. C. Chang,² R. S. Liu,² J. M. Lee,^{1,3} M. Park,⁴ and J. H. Choy⁴

¹National Synchrotron Radiation Research Center (NSRRC), Hsinchu 30077, Taiwan, Republic of China

²Department of Chemistry, National Taiwan University, Taipei 106, Taiwan, Republic of China

³Department of Electrophysics, National Chiao Tung University, Hsinchu 30077, Taiwan, Republic of China

⁴National Nanohybrid Materials Laboratory, School of Chemistry, Seoul National University, Seoul 151-747, Korea

(Received 17 May 2004; revised manuscript received 22 September 2004; published 4 March 2005)

Unoccupied electronic states of $X\text{-Bi}_2\text{Sr}_2\text{CaCu}_2\text{O}_8$ [$X=\text{I}$, HgI_2 , and $(\text{Py-CH}_3)_2\text{HgI}_4$, $\text{Py}=\text{pyridine}$] have been probed by O K -edge and Cu L -edge x-ray absorption near-edge structure (XANES) spectra using a bulk-sensitive x-ray-fluorescence-yield technique. In the O $1s$ absorption edge of $X\text{-Bi}2212$, the pre-edge feature at ~ 528.3 eV is attributed to transitions into O $2p$ hole states located in the CuO_2 planes. As deduced from O K -edge and Cu L -edge x-ray absorption spectra, the hole concentration in the CuO_2 planes of $X\text{-Bi}2212$ increases for $X=\text{I}$ and HgI_2 , but decreases for $X=(\text{Py-CH}_3)_2\text{HgI}_4$, relative to pristine $\text{Bi}2212$. The present XANES results clearly demonstrate that the hole density within the CuO_2 planes of intercalated $\text{Bi}_2\text{Sr}_2\text{CaCu}_2\text{O}_8$ can be not only decreased but also increased, depending on the chemical character of the intercalants.

DOI: 10.1103/PhysRevB.71.094501

PACS number(s): 78.70.Dm, 74.72.-h

I. INTRODUCTION

The intercalation of guest molecules into high- T_c superconductive copper-oxide materials has received much attention recently because of practical application of high- T_c superconductors.^{1,2} Several new high- T_c intercalated superconductors, such as $\text{La}_2\text{CuO}_{4-\delta}\text{F}_y$,^{3,4} $\text{Sr}_2\text{CuO}_2\text{F}_{2+\delta}$,⁵ $\text{HgBa}_2\text{Sr}_2\text{Cu}_2(\text{CO}_3)\text{O}_7$,⁶ $(\text{Hg}_{0.3}\text{Pb}_{0.7})\text{Sr}_4\text{Cu}_2(\text{CO}_3)\text{O}_7$,⁷ $(\text{Tl}_{0.5}\text{Pb}_{0.5})\text{Sr}_4\text{Cu}_2(\text{CO}_3)\text{O}_7$,⁸ $(\text{Bi}_{0.5}\text{Hg}_{0.5})\text{Sr}_4\text{Cu}_2(\text{CO}_3)\text{O}_7$,⁹ $\text{HgBa}_2\text{Ca}_{n-1}\text{Cu}_n\text{O}_{2n+2+\delta}\text{F}_y$ ($n=1-3$),¹⁰ and $X\text{-Bi}_2\text{Sr}_2\text{Ca}_{m-1}\text{Cu}_m\text{O}_y$ [$m=1$ and 2 ; $X\text{-Bi}2201$ and $X\text{-Bi}2212$; $X=\text{I}$, HgI_2 , $(\text{Me}_3\text{S})_2\text{HgI}_4$, and $(\text{Py-C}_n\text{H}_{2n+1})_2\text{HgI}_4$, $n=1-12$, $\text{Py}=\text{pyridine}$]^{11,12}, have been reported. Among them, $X\text{-Bi}2212$ or $X\text{-Bi}2201$ systems have attracted extensive investigation because of their unique properties and controversial issues regarding the role of interlayer coupling on superconductivity.¹¹⁻¹⁵

Pristine $\text{Bi}2212$ and $\text{Bi}2201$ exhibit weakly bound Bi-O double layers, enabling free expansion of the unit cell in the c direction without significantly changing other internal structure of the lattice.^{11,12} Various inorganic or organic modulation layers have been intercalated into Bi_2O_2 double layers of these $\text{Bi}2201$ and $\text{Bi}2212$ materials. In particular, long-chain organic molecules, such as $(\text{Py-C}_n\text{H}_{2n+1})_2\text{HgI}_4$ with $n=1-12$, were successfully intercalated into Bi -based cuprates in the form of a complex heterostructured high- T_c superconducting nanohybrid.¹¹ Relative to pristine $\text{Bi}2212$, the onset T_c value increases slightly upon $(\text{Py-CH}_3)_2\text{HgI}_4$ intercalation, whereas T_c decreases ~ 10 K upon intercalation of mercury (II) iodide and by ~ 15 K upon intercalation of iodine.^{11,12} Elucidation of the origin of this variation of T_c through various intercalants into $\text{Bi}_2\text{Sr}_2\text{CaCu}_2\text{O}_8$ is of interest so as to gain profound insight into the mechanism of the appearance of high- T_c superconductivity. One possible factor is the structural change along the c axis; another is the variation of the hole concentration in the CuO_2 sheets through intercalation.

Several techniques have been widely utilized to estimate the hole concentration for cuprate superconductors, including the Hall coefficient measurement, calculation of the bond-valence sum,¹⁶ iodometric titration,^{17,18} soft-x-ray absorption spectroscopy,^{18,19} and thermoelectric power measurement.²⁰ Among them, soft-x-ray absorption spectroscopy using synchrotron radiation offers advantages over other measurements. The x-ray absorption near-edge structure (XANES) spectrum at the O K -edge and Cu $L_{2,3}$ -edge directly probes the local concentration of hole carriers at distinct oxygen and copper sites in superconductive cuprate materials.¹⁸

Based on extended x-ray absorption fine-structure (EXAFS) measurements at the Bi I L_3 -edge, Cu K -edge, I L_1 -edge, and Hg L_3 -edge for $\text{Bi}2212$, $\text{HgI}_2\text{-Bi}2212$, and $(\text{Me}_3\text{S})_2\text{HgI}_4\text{-Bi}2212$, it has been proposed that the T_c evolution of $\text{Bi}2212$ and its intercalates is related mainly to the variation of the hole concentration in the CuO_2 planes.¹² To understand further the mechanism of high- T_c superconductivity, it is crucially important to probe directly the hole density of intercalated cuprates with various interlayer distances. In this study, the unoccupied electronic states for $\text{Bi}2212$ and $X\text{-Bi}2212$ [$X=\text{I}$, HgI_2 , and $(\text{Py-CH}_3)_2\text{HgI}_4$] have been probed by O K -edge and Cu L -edge x-ray absorption spectra using a bulk-sensitive x-ray fluorescence yield. Our XANES results demonstrate clearly that the hole density in the CuO_2 planes of intercalated $\text{Bi}_2\text{Sr}_2\text{CaCu}_2\text{O}_8$ can be both decreased and increased, depending on the chemical character of the intercalants.

II. EXPERIMENTS

The polycrystalline $\text{Bi}2212$ compound was prepared through conventional solid-state reaction. Detailed procedures for preparing superconducting $X\text{-Bi}_2\text{Sr}_2\text{CaCu}_2\text{O}_8$ [$X=\text{I}$, HgI_2 , and $(\text{Py-CH}_3)_2\text{HgI}_4$] are reported elsewhere.^{11,12} In brief, I- and HgI_2 -intercalated $\text{Bi}2212$ compounds were prepared on heating the pristine materials and the guest iodine

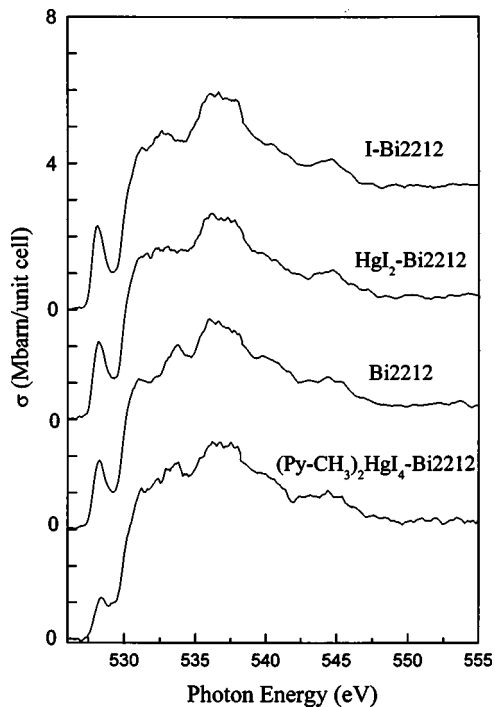


FIG. 1. O K -edge x-ray-fluorescence-yield absorption spectra of I-Bi2212, HgI₂-Bi2212, Bi2212, and (Py-CH₃)₂HgI₄-Bi2212.

or HgI₂, respectively, in a Pyrex tube sealed under vacuum. Intercalation of the organic molecules was performed through the solvent-mediated reaction between HgI₂-intercalated Bi2212 and methyl-pyridinium iodide. As verified by powder x-ray diffraction (XRD) analysis and high-resolution electron-microscopy (HREM) images, all samples for the present work are single phase.¹¹

X-ray absorption measurements were performed at the 6-m high-energy spherical-grating-monochromator (HSGM) beamline of the National Synchrotron Radiation Research Center (NSRRC) in Taiwan. X-ray absorption spectra were recorded in the x-ray-fluorescence-yield mode using a micro-channel plate detector. The x-ray-fluorescence-yield measurement is sensitive strictly to the bulk of a sample because the probing depth is hundreds of nm. The fluorescence detector was oriented parallel to the sample surface. Photons were incident at an angle 45° with respect to the sample normal. The incident photon flux (I_0) was monitored simultaneously with an Au mesh located after the exit slit of the monochromator. The x-ray-fluorescence-yield absorption spectra were corrected for both the energy-dependent incident photon intensity and the self-absorption effects, and normalized to a tabulated standard absorption cross section in the energy range 600-620 eV at the O K -edge and 1000 - 1020 eV at the Cu $L_{2,3}$ -edge. The photon energies were calibrated with an accuracy 0.1 eV using the known O K -edge absorption feature at 530.1 eV and the Cu L_3 white line at 931.2 eV of a CuO reference. The monochromator resolution was set at ~ 0.22 eV and ~ 0.45 eV at the O K -edge and Cu $L_{2,3}$ -edge, respectively.

III. RESULTS AND DISCUSSION

In Fig. 1, the O K -edge x-ray absorption spectra for

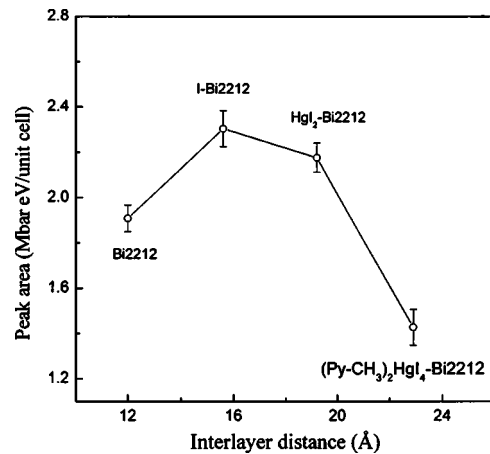


FIG. 2. Hole content in the CuO₂ planes as a function of interlayer distance between the CuO₂ planes in adjacent blocks of pristine Bi2212, I-Bi2212, HgI₂-Bi2212, and (Py-CH₃)₂HgI₄-Bi2212.

Bi2212 and X -Bi2212 [X =I, HgI₂, and (Py-CH₃)₂HgI₄] are depicted. The core-hole effect in the O K -edge absorption spectrum can be neglected, because of the strong similarity of O $1s$ absorption edges and resonant inverse photoemission spectra of Bi2212.²¹ The O K -edge absorption spectrum thus probes the local unoccupied density of states with p symmetry at the O sites. Based on polarization-dependent O K -edge x-ray absorption spectra of pristine Bi2212 and HgI₂-Bi2212 single crystals, the pre-edge peak at ~ 528.3 eV in Fig. 1 has mainly O $2p_{xy}$ symmetry and is ascribed to holes in the singlet band formed on p -type doping in the CuO₂ planes, i.e., the Zhang-Rice (ZR) states.²²⁻²⁴ A similar feature has been characterized for many other p -type doped superconductive cuprates.²⁵⁻²⁷ The feature at ~ 530.5 eV is due to overlapping of wide antibonding Bi $6p$ -O $2p$ and the upper Hubbard band (UHB).^{18,19} The absorption energy of the ZR band slightly decreases with increasing intensity of the ZR band. This effect demonstrates that the Fermi level is shifted to lower energy when the hole concentration within the CuO₂ planes increases.

To quantify the results in Fig. 1, we analyzed the spectral weight of pre-edge features by fitting with Gaussian functions. The energy shift of ZR bands upon intercalation in Bi2212 was taken into consideration. The resulting hole content in the CuO₂ planes as a function of interlayer distance between the CuO₂ planes in adjacent blocks of pristine Bi2212 and various intercalates is shown in Fig. 2. As is discernible from Fig. 2, the hole concentration in the CuO₂ planes of X -Bi2212 increases for X altering from HgI₂ to I, but decreases for X =(Py-CH₃)₂HgI₄, relative to pristine Bi2212. As noted, the variation of hole concentration in the CuO₂ planes of X -Bi2212 is insensitive to the interlayer distance between the CuO₂ planes. The present XANES results demonstrate clearly that the CuO₂-plane hole concentration of intercalated Bi2212 can be not only decreased but also increased, depending on the chemical nature of the intercalants.

Organic or inorganic molecules become intercalated between B₂O₂ layers in Bi2212.¹¹ Hence, in these intercalated Bi-based cuprates, the Bi-O plane directly faces the intercal-

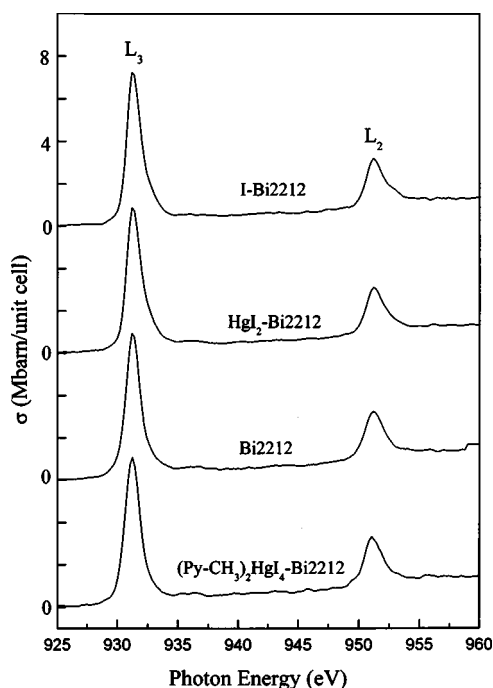


FIG. 3. Cu $L_{2,3}$ -edge x-ray absorption spectra of I-Bi2212, HgI_2 -Bi2212, Bi2212, and $(\text{Py-CH}_3)_2\text{HgI}_4$ -Bi2212.

ant layer. It is generally believed that hole doping of the CuO_2 planes in Bi2212 reflects charge transfer from the CuO_2 planes to the BiO planes through internal redox equilibrium $\text{Bi(III)} + \text{Cu(II)} \leftrightarrow \text{Bi(III}-\epsilon) + \text{Cu(II} + \epsilon)$.^{12,19} Accordingly, the hole density in the CuO_2 plane is modified by the redox of the Bi-O layer in close contact with the intercalated guests. The chemical interaction between host and guest of intercalated Bi2212 is primarily affected by the relative electron donating or accepting ability involving the orbitals of Bi-O layers and guest molecules. Calculations based on the extended Hückel tight-binding band method have determined the relative energy levels of molecular orbitals in the $\text{Bi}_2\text{O}_4^{2-}$ cluster, HgI_2 , and HgI_4^{2-} .¹² For HgI_2 -intercalated Bi2212, the HOMO of $\text{Bi}_2\text{O}_4^{2-}$ acts as a donor orbital and the LUMO of HgI_2 as an acceptor orbital. Electrons are thereby preferably transferred from the $\text{Bi}_2\text{O}_4^{2-}$ cluster to the HgI_2 layer upon intercalation, and in turn the Bi-O layer becomes slightly oxidized. In contrast, for HgI_4^{2-} -intercalated Bi2212, the HOMO of HgI_4^{2-} behaves as a donor orbital and the LUMO of $\text{Bi}_2\text{O}_4^{2-}$ as an acceptor orbital, leading to partial electron transfer from the HgI_4^{2-} anion to a $\text{Bi}_2\text{O}_4^{2-}$ cluster, i.e., to the Bi-O sheet. Such theoretical predictions are consistent with the present O K -edge XANES spectra.

If the T_c variation of pristine Bi2212 upon intercalation is attributed to a weakening of interblock coupling due to the basal increment, T_c is expected to decrease monotonically with increasing basal increment regardless of the hole concentration.¹³ However, in contrast to theoretical prediction, relative to pristine Bi2212, the onset T_c value increases slightly despite a basal increment ($\Delta d \approx 10.9 \text{ \AA}$) upon $(\text{Py-CH}_3)_2\text{HgI}_4$ intercalation, whereas T_c decreases $\sim 10 \text{ K}$ upon intercalation of HgI_2 ($\Delta d \approx 7.2 \text{ \AA}$) and by $\sim 15 \text{ K}$ upon intercalation of iodine ($\Delta d \approx 3.6 \text{ \AA}$).^{11,12} It has been shown that

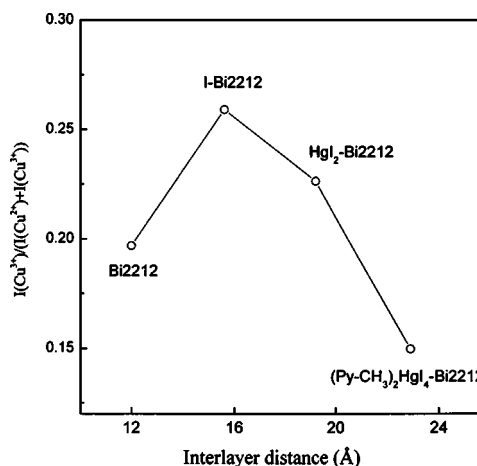


FIG. 4. Normalized intensity, $I(\text{Cu}^{3+})/[I(\text{Cu}^{2+}) + I(\text{Cu}^{3+})]$, as a function of interlayer distance between the CuO_2 planes in adjacent blocks of pristine Bi2212, I-Bi2212, HgI_2 -Bi2212, and $(\text{Py-CH}_3)_2\text{HgI}_4$ -Bi2212.

T_c as a function of hole concentration in the CuO_2 planes conforms to a parabolic curve for many p -type high- T_c cuprate superconductors.²⁸ $\text{Bi}_2\text{Sr}_2\text{CaCu}_2\text{O}_8$ is situated in the overdoped region in which an increased hole concentration in the CuO_2 planes produces a decreased T_c .¹⁸ Thus HgI_2 - and I-intercalated Bi2212 depress T_c for overdoped pristines, corresponding to the hole doping from intercalant layers to CuO_2 sheets. In contrast, the T_c recovery upon $(\text{Py-CH}_3)_2\text{HgI}_4$ intercalation is attributed to a decreased hole density in the CuO_2 planes upon attaining an optimum hole concentration, originating from charge transfer from intercalant sheets to the CuO_2 layer in host materials. Our present XANES results clearly demonstrate that the variation of hole concentration in the CuO_2 planes is primarily responsible for the variation of T_c upon intercalation.

In Fig. 3, the Cu $L_{2,3}$ -edge x-ray-fluorescence-yield absorption spectra of pristine Bi2212 and X -Bi2212 [$X = \text{I}, \text{HgI}_2$, and $(\text{Py-CH}_3)_2\text{HgI}_4$] in the energy range 925 - 960 eV are reproduced. As noted, the Cu L -edge absorption spectrum exhibits an asymmetric profile with a tail extending to higher energies. Two excitonic features centered at $\sim 931.2 \text{ eV}$ and $\sim 951.2 \text{ eV}$ are ascribed to transitions from the $\text{Cu}(2p_{3/2,1/2})3d^9 - \text{O } 2p^6$ ground state (formally Cu^{2+}) into the $\text{Cu}(2p_{3/2,1/2})^{-1}3d^{10} - \text{O } 2p^6$ excited state, in which $(2p_{3/2,1/2})^{-1}$ represents a $2p_{3/2}$ or $2p_{1/2}$ hole. The high-energy shoulders in Fig. 3 originating from O $2p$ hole states are ascribed to transitions from the $\text{Cu}(2p_{3/2,1/2})3d^9L$ ground state into the $\text{Cu}(2p_{3/2,1/2})^{-1}3d^{10}L$ excited state (formally Cu^{3+}), with L denoting a ligand hole in the O $2p$ orbital.^{18,29-32}

We analyzed the absorption spectra in Fig. 3 by fitting the Cu L_3 peak and its shoulder with Gaussian functions. The integrated intensity of the shoulder $I(\text{Cu}^{3+})$ is normalized against the sum of integrated intensity of the main feature $I(\text{Cu}^{2+})$ and that of the shoulder itself. The normalized intensity of the shoulder, i.e., $I(\text{Cu}^{3+})/[I(\text{Cu}^{2+}) + I(\text{Cu}^{3+})]$, enables an estimate of the hole concentration in the CuO_2 planes, like the pre-edge peak at $\sim 528.3 \text{ eV}$ observed in the O K -edge x-ray absorption spectrum.²⁶ In Fig. 4, the obtained normal-

ized intensity of the shoulder is plotted as a function of interlayer distance between the CuO_2 planes in adjacent blocks of pristine Bi2212 and various intercalates. The normalized intensity of the shoulder increases upon intercalation with HgI_2 and iodine and decreases after intercalation with $(\text{Py-CH}_3)_2\text{HgI}_4$ into Bi2212 . This result is consistent with O K -edge absorption spectra in Fig. 1.

IV. CONCLUSION

We have investigated the variation of hole density of Bi2212 and $X\text{-Bi2212}$ [$X=\text{I}$, HgI_2 , and $(\text{Py-CH}_3)_2\text{HgI}_4$] with high-resolution O K -edge and Cu L -edge x-ray absorption spectra. Relative to pristine Bi2212 , the hole concentration in the CuO_2 planes for I- and HgI_2 -intercalated Bi2212 increases, decreasing T_c through overdoping of holes in the CuO_2 planes. The recovery of T_c upon intercalation of $(\text{Py-CH}_3)_2\text{HgI}_4$ into Bi2212 is ascribed to a decreased hole concentration in the CuO_2 planes upon attaining an optimum hole concentration. The present XANES results demonstrate clearly that the hole density within the CuO_2 planes of intercalated $\text{Bi}_2\text{Sr}_2\text{CaCu}_2\text{O}_8$ can be both decreased and increased, depending on the chemical character of the intercalants. The variation of CuO_2 -plane hole concentration of Bi2212 is primarily responsible for the T_c variation upon intercalation.

ACKNOWLEDGMENTS

We gratefully acknowledge the technical support of the NSRRC staff. This work is supported by the NSRRC and the National Science Council of the Republic of China (Grants No. NSC 92-2113-M-213-007 and No. NSC 92-2113-M-002-036). J.H.C. and M.P. would like to express their thanks for the financial support from the National Research Laboratory (NRL) project '99 and Brain Korea 21 Program.

*Author to whom correspondence should be addressed.

- ¹X. D. Xiang, W. A. Vareka, A. Zettl, J. L. Corkill, T. W. Barbee III, M. L. Cohen, N. Kijima, and R. Gronsky, *Science* **254**, 1487 (1991).
- ²J. H. Choy, S. J. Hwang, and N. G. Park, *J. Am. Chem. Soc.* **119**, 1624 (1997).
- ³M. H. Tuilier, B. Chevalier, A. Tressaud, C. Brisson, J. L. Soubeyroux, and J. Etourneau, *Physica C* **200**, 113 (1992).
- ⁴V. Bhat and J. M. Honig, *Mater. Res. Bull.* **30**, 1253 (1995).
- ⁵M. Al-Mamouri, P. P. Edwards, C. Greaves, and M. Slaski, *Nature (London)* **369**, 382 (1994).
- ⁶M. Uehara, S. Sahoda, H. Nataka, J. Akimitsu, and Y. Matsui, *Physica C* **222**, 27 (1994).
- ⁷C. Martin, A. Maignan, M. Hervieu, M. Huve, C. Michel, A. Maigann, G. Van Tendeloo, and B. Raveau, *Physica C* **222**, 19 (1994).
- ⁸M. Huve, C. Michel, A. Maignan, M. Hervieu, C. Martin, and B. Raveau, *Physica C* **205**, 219 (1993).
- ⁹D. Pelloquin, M. Hervieu, C. Michel, A. Maignan, and B. Raveau, *Physica C* **227**, 215 (1994).
- ¹⁰M. Marezio, J. J. Capponi, P. G. Radaelli, P. P. Edwards, A. R. Armstrong, and W. I. F. David, *Eur. J. Solid State Inorg. Chem.* **31**, 843 (1994).
- ¹¹J. H. Choy, S. J. Kwon, and G. S. Park, *Science* **280**, 1589 (1998).
- ¹²S. J. Kwon, J. H. Choy, D. Jung, and P. V. Huong, *Phys. Rev. B* **66**, 224510 (2002).
- ¹³J. M. Wheatley, T. C. Hsu, and P. W. Anderson, *Nature (London)* **333**, 121 (1988).
- ¹⁴D. R. Harshman and A. P. Mills, *Phys. Rev. B* **45**, 10 684 (1992).
- ¹⁵M. Di Stasio, K. A. Muller, and L. Pietronero, *Phys. Rev. Lett.* **64**, 2827 (1990).
- ¹⁶J. J. Capponi, C. Chaillout, A. W. Hewat, P. Lejay, M. Marezio, N. Nguyen, B. Raveau, J. L. Soubeyroux, J. L. Tholence, and R. Tournier, *Europhys. Lett.* **3**, 1301 (1987).
- ¹⁷M. W. Shafer, T. Penney, and B. L. Olson, *Phys. Rev. B* **36**, 4047 (1987).
- ¹⁸M. Karppinen, M. Kotiranta, T. Nakane, H. Yamauchi, S. C. Chang, R. S. Liu, and J. M. Chen, *Phys. Rev. B* **67**, 134522 (2003).
- ¹⁹J. Fink, N. Nücker, E. Pellegrin, H. Romberg, M. Alexander, and M. Knupfer, *J. Electron Spectrosc. Relat. Phenom.* **66**, 395 (1994).
- ²⁰S. D. Obertelli, J. R. Cooper, and J. L. Tallon, *Phys. Rev. B* **46**, 14928 (1992).
- ²¹W. Drube, F. J. Himpsel, G. V. Chandrashekar, and M. W. Shafer, *Phys. Rev. B* **39**, 7328 (1989).
- ²²R. K. Singhal, N. L. Saini, B. Dalela, S. Dalela, J. H. Choy, D. Charturved, B. R. Sekhar, D. C. Jain, K. B. Garg, H. J. Lin, T. Y. Hou, and C. T. Chen, *J. Phys.: Condens. Matter* **14**, 6675 (2002).
- ²³N. Nücker, H. Romberg, X. X. Xi, J. Fink, B. Gegenheimer, and Z. X. Zhao, *Phys. Rev. B* **39**, 6619 (1989).
- ²⁴O. Tjernberg, H. Nylén, G. Chiaia, S. Söderholm, U. O. Karlsson, M. Qvarford, I. Lindau, C. Puglia, N. Mårtensson, and L. Leonnyuk, *Phys. Rev. Lett.* **79**, 499 (1997).
- ²⁵N. Nücker, E. Pellegrin, P. Schweiss, J. Fink, S. L. Molodtsov, C. T. Simmons, G. Kaindl, W. Frentrup, A. Erb, and G. Müller-Vogt, *Phys. Rev. B* **51**, 8529 (1995).
- ²⁶J. M. Chen, R. S. Liu, and W. Y. Liang, *Phys. Rev. B* **54**, 12587 (1996).
- ²⁷M. Karppinen, M. Kotiranta, H. Yamauchi, P. Nachimuthu, R. S. Liu, and J. M. Chen, *Phys. Rev. B* **63**, 184507 (2001).
- ²⁸J. L. Tallon, C. Bernhard, H. Shaked, R. L. Hitterman, and J. D. Jorgensen, *Phys. Rev. B* **51**, 12 911 (1995).
- ²⁹A. Bianconi, M. De Santis, A. Di Cicco, A. M. Flank, A. Fontaine, P. Lagarde, H. Katayama-Yoshida, A. Kotani, and A. Marcelli, *Phys. Rev. B* **38**, 7196 (1988).
- ³⁰A. Q. Pham, F. Studer, N. Merrien, A. Maignan, C. Michel, and B. Raveau, *Phys. Rev. B* **48**, 1249 (1993).
- ³¹N. L. Saini, D. S.-L. Law, P. Pudney, K. B. Garg, A. A. Menovsky, and J. J. M. Franse, *Phys. Rev. B* **52**, 6219 (1995).
- ³²P. Ghigna, G. Spinolo, G. Flor, and N. Morgante, *Phys. Rev. B* **57**, 13 426 (1998).